Journal of Applied Polymer Science

Synthesis of Poly(butyl acrylate)-Poly(methyl methacrylate) Core–Shell Nanomaterials of Anti-Crease-Whitening Properties

Wenjing Zhang,[1] Luye Mu,[2] Yun Wang,[3] Shaohui Lin,[1] Qinmin Pan[1]
[1]Green Polymer and Catalysis Technology Laboratory, Soochow University, Suzhou 215123, China
[2]Waterloo Institute for Nanotechnology, University of Waterloo, Waterloo, ON N2L 3G1, Canada
[3]Zhejiang Reflective Materials Co. Ltd., Taizhou 318000, China
Correspondence to: Q. Pan (E-mail: qpan@suda.edu.cn).

ABSTRACT: Core–shell nanomaterials of poly(butyl acrylate)-poly(methyl methacrylate) were synthesized using a differential microemulsion polymerization method for being used as polyacrylate-based optical materials, which meet the requirement of anti-crease-whitening and proper mechanical strength. The effects of reaction temperature and surfactant amount on the particle sizes, as well as the effect of reaction temperature on the conversion and solid content were investigated to reveal the dependence of the application properties on the reaction conditions. The spherical morphology of core–shell nanoparticles was also studied via transmission electron microscopy. The resulting polymers with a core–shell monomer ratio of butyl acrylate/methyl methacrylate at 32/10 (vol/vol) demonstrated the optimal balanced properties in the anti-crease-whitening and mechanical property, confirmed by the visible light transmittance measurement and the dynamic analysis of the viscoelastic properties of the synthesized core–shell nanomaterials. The smaller the particle size, the better the transparency of the resulting polymer films. © 2013 Wiley Periodicals, Inc. J. Appl. Polym. Sci. **2014**, *131*, 39991.

KEYWORDS: emulsion polymerization; morphology; nanostructured polymers

Received 23 May 2013; accepted 22 September 2013
DOI: 10.1002/app.39991

INTRODUCTION

Anti-crease-whitening of polymer materials is an important property when these materials are used for optical components.[1] However, how to modify a polymer in order to achieve such a property has not yet been extensively investigated. To date, the major approaches used to overcome polymer crease-whitening include grafting the polymers with rubber,[2] or blending the polymers with rubber, clay, or fiber.[3–6] LG Chemical Company[2] invented an technical route by conducting three steps of grafting polymerization to prepare methylmethacrylate-butadiene-styrene copolymer with superior impact resistance, transparency, and anti-stress-whitening. Hadal et al.[5] found that clay-reinforced polybutene and polymethylpentene nanocomposite systems had significantly reduced stress-whitening phenomenon.

Core–shell structured materials with different composite domains in the cores and shells have received increasing attention for their superior performance compared to polymer blends and copolymers.[7] Using different polymers in the cores and shells, a composite with properties distinct from those of its pure constituents can be made. Such composite materials are widely used in various areas. For example, polymer–polymer core–shell particles can be used as effective structures for applications in pigments,[7] fibers,[8] immunological studies,[9] drug delivery systems,[10] baroplastic processing,[11] toughening polymeric materials,[12–14] transparent conductive thin films,[15] coatings,[16] and adhesives.[17,18] The combined properties of core and shell polymers are superior to mechanical blends of those polymers. In addition, polymer-inorganic core–shell structured materials can be applied as specific functional composites, which have not only high mechanical strength but also excellent physical, chemical, or biological properties.[19–26] Thus, engineering core–shell structures with proper combinations of compositions, such as hard components, soft components, and tough components, would be a feasible approach to overcome the crease-whitening of polymer materials.

Various techniques have been developed for preparing polymer core–shell structures during last decade. These methods include seeded emulsion polymerization,[27–31] seeded dispersion polymerization,[32] stepwise heterocoagulation method,[33,34] and emulsifier-free emulsion polymerization.[35,36] Furthermore, surface-initiated living radical polymerization[37] and layer-by-layer deposition[38] have also succeeded in achieving well-defined core–shell morphologies. Particularly, the two-stage method of seeded emulsion polymerization is a typical method that commonly adopts batch and semi-batch manner in two stages.

Furthermore, to minimize the amount of the surfactant that is needed for reducing the particle size, a method called differential microemulsion polymerization was proposed,[39] which allowed the preparation of small particles with very a small surfactant/monomer weight ratio.[39–45]

Acrylate-based polymers are widely involved in optical applications for their transparency and weather resistance.[46,47] However, they exhibit poor anti-crease-whitening, and there are very few reports to date that target overcoming the crease-whitening problem of acrylate-based polymers. The crucial requirement is that while achieving the anti-crease-whitening property of a polymer material the other mechanical properties of the polymer material should not be compromised. Thus, in this study, we sought to prepare core–shell acrylate polymer materials with both anti-crease-whitening property and proper mechanical property, and poly(butyl acrylate) (PBA) and poly(methyl methacrylate) (PMMA) based anti-crease-whitening materials were pursued.

There have been a few research reports on the synthesis of PBA-PMMA core–shell structures, although they were not for the purpose of improving anti-crease-whitening. For example, Moghbeli and Tolue[48] synthesized PBA-PMMA core–shell particles with average diameters from 100 to 170 nm via two-stage seeded emulsion polymerization for the purpose of being used as a modifier of particulate flow and toughening of polyvinyl chloride. Udagama and Mckenna[49] prepared PBA-PMMA core–shell particles with diameters around 200 nm via seeded emulsion polymerization for the purpose of obtaining low-viscosity and high solid content latex products. However, no information was provided regarding the transparency and the anti-crease-whitening property.

In this article, not only the synthesis of the core–shell structured PBA-PMMA was studied, but also the mechanical and anti-crease-whitening properties were investigated.

EXPERIMENTAL

Materials

Butyl acrylate (BA) (CP grade, Sinopharm Chemical Reagent Co., China) and methyl methacrylate (MMA) (CP grade, Sinopharm Chemical Reagent Co., China) were used as received. Sodium dodecyl sulfate (SDS) (Purity $\geq$ 86%, Sinopharm Chemical Reagent Co., China) was used as the surfactant and potassium persulfate (KPS) (AR grade, Sinopharm Chemical Reagent Co., China) was used as the initiator. SDS, KPS, and calcium chloride anhydrous (AR grade, purity $\geq$ 96%, Sinopharm Chemical Reagent Co., China) were used without further purification. Deionized water was used as reaction media in all experiments.

Synthesis of Core–Shell Nanoparticles

Polymerizations were conducted in a 250-mL four-necked jacketed glass flask reactor equipped with a mechanical stirrer. Stirring was kept constant at the speed of 200 rpm throughout the reaction. The reaction system was purged with nitrogen for 30 min to remove oxygen before the reaction was initiated. SDS and KPS were dissolved in water and the system was heated to 80°C, and then BA was added in a differential manner[39] for about 2 h. The reaction system was then kept at 80°C for 2 h to obtain core polymer particles. Before the shell polymerization stage, additional KPS was added into the reactor. With the temperature maintained at 80°C, MMA was added slowly in approximately 1 h to limit the shell monomer concentration within a differential amount in the reaction system. Afterwards, the reaction was conducted for 4 h before being cooled down to room temperature.

The resultant core–shell polymers were precipitated using a saturated calcium chloride solution and were separated by a vacuum filtration technique. The precipitate was washed three times with deionized water to remove surfactant, initiator, and calcium chloride. Then core–shell polymers were dried at ambient temperature in a vacuum drying oven for 24 h.

Characterization of PBA-PMMA Core–Shell Polymer

The solid content and monomer conversion were determined by gravimetric analysis. Samples were dried in an oven at 60°C to constant weight. The calculation methods are as follows:

$$\text{Solid content} = {}^{W_1}\!/_{W_2} \times 100\%$$

where W_1 and W_2 are the mass of the dry product and latex, respectively.

$$\text{Monomer conversion} = {}^{(W_1 - W_3)}\!/_{W_4} \times 100\%$$

where W_3 is the total mass of KPS and SDS, and W_4 is the total mass of BA and MMA that were added to the reaction.

The Z-average particle size, particle size distribution, and zeta-potential of the latex were measured by dynamic light scattering (Malvern Zetasizer Nano ZS, UK) at 25°C.

The glass transition temperature (T_g) of dried samples was measured by differential scanning calorimetry (DSC, TA 2000, USA). The scanning rate applied was 10°C/min from −80°C to 180°C.

The morphology of the latex particles was obtained by transmission electron microscopy (TEM, FEI Tecnai G220, USA).

The surface morphologies of the resultant polymer films were studied using a scanning electron microscope (SEM, Hitachi S-4700, Japan) at an accelerating voltage of 15 kV.

The polymer films were tested via ultraviolet and visible spectroscopy (Shimadzu UV 3150, Japan) for their transmittance. About 2 mL of each emulsion was directly coated on a clean glass substrate, which formed around 0.1 mm thick films at room temperature after drying.

The dynamic mechanical analysis (DMA) experiments were performed in a DMA Q800 analyzer in the extension mode with temperature ramp rate of 5°C/min from −80°C to 150°C at 1 Hz.

RESULTS AND DISCUSSION

Effect of Reaction Temperature on Particle Size, Monomer Conversion, and Solid Content

The experimental data in Figure 1 show that the core and core–shell particle size decreased with the reaction temperature rising from 75°C to 85°C, although the size decreasing was not

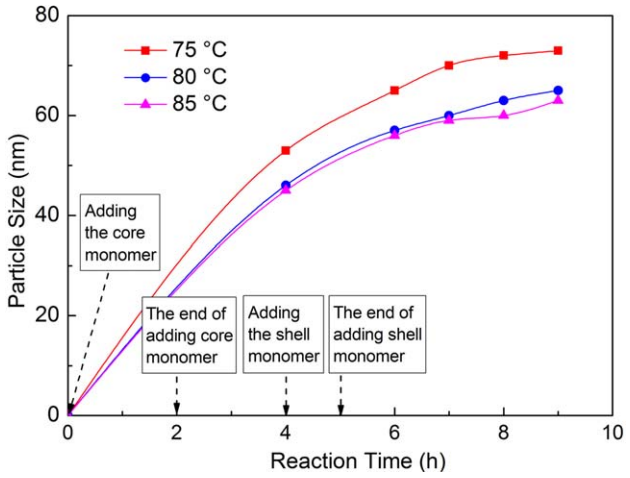

Figure 1. Particle size versus reaction time with various temperatures (Core stage: 32 mL BA, 0.15 g KPS, 0.6 g SDS, 90 mL water; Shell stage: 10 mL MMA, 0.05 g KPS dissolved in 10 mL of water). [Color figure can be viewed in the online issue, which is available at wileyonlinelibrary.com.]

significant from 80°C to 85°C. The possible reason is that higher temperature resulted in an increase in the decomposition rate of the initiator to form more free radicals. Consequently, the polymerization rate and nucleation rate both increased, which resulted in an increase in the particles number, and a decrease in the particle size.

It can be seen from Figure 2 that the monomer conversion and solid content both increased with the reaction temperature. With an increase in the reaction temperature from 75°C to 80°C, the core–shell monomer conversion increased from 92% to 96% and the solid content from 26% to 28%, respectively. However, the effect of the reaction temperature on the conversion and solid content was not significant between 80°C and 85°C. Therefore, combined with the effect of the temperature on the particle size discussed above, 80°C was chosen as the optimal reaction temperature for further detailed investigation.

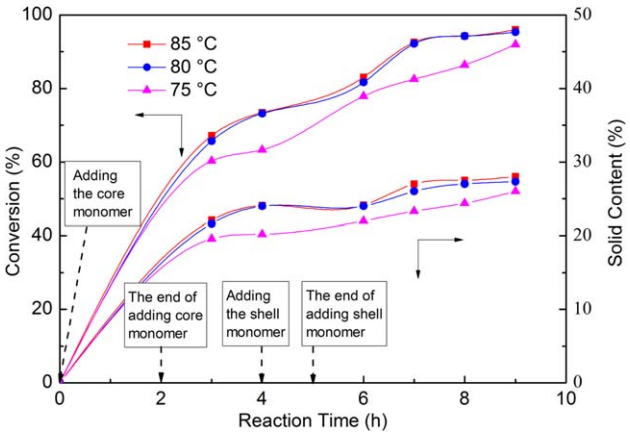

Figure 2. Conversion and solid content versus time with various temperatures (Core stage: 32 mL BA, 0.15 g KPS, 0.6 g SDS, 90 mL water; Shell stage: 10 mL MMA, 0.05 g KPS dissolved in 10 mL of water). [Color figure can be viewed in the online issue, which is available at wileyonlinelibrary.com.]

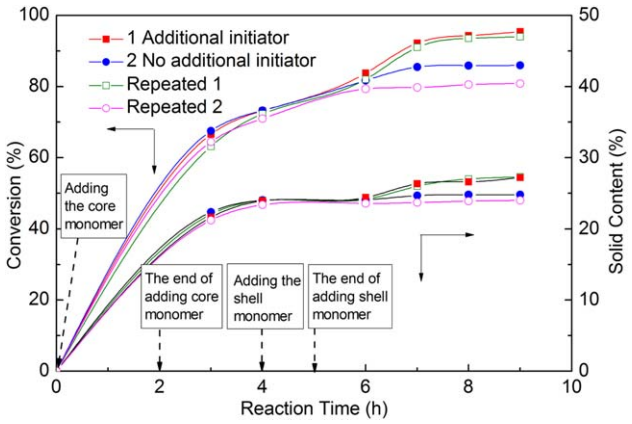

Figure 3. Effect of additional initiator at the shell polymerization stage on conversion and solid content (Core stage: 32 mL BA, 0.15 g KPS, 0.6 g SDS, 90 mL water, 80°C; Shell stage: (1) 10 mL MMA, 0.05 g KPS dissolved in 10 mL of water, 80°C. (2) 10 mL MMA, 80°C). [Color figure can be viewed in the online issue, which is available at wileyonlinelibrary.com.]

Effect of Additional Initiator on Conversion and Solid Content

Figure 3 presents the influence of adding initiator at the shell polymerization stage on the conversion and solid content. Compared with the results obtained without introducing additional initiators at the shell polymerization stage, the conversion and solid content was increased in the former. Therefore, adding additional initiator at the shell polymerization stage was helpful in promoting the completion of the shell formation. To validate the reliability of the experiments, repeated experiments were also conducted, and they demonstrated satisfactory repeatability, as shown in Figure 3.

Effect of Weight Ratio of Surfactant/Total Monomer on Particle Size

The amount of surfactant played an important role in determining the particle size in core–shell polymerization. Figure 4 shows that the core and core–shell particle size decreased with an increase in the weight ratio of surfactant/monomers from 7.85×10^{-3} to 1.83×10^{-2}. When the SDS concentration in water exceeded the critical micelle concentration, micelles and the nucleation sites would be generated. Higher SDS concentration allowed the creation of more micelles, yielding smaller particle sizes. Figure 4 indicates that when the weight ratio of surfactant/monomers was 1.83×10^{-2}, the core and core–shell particle sizes were 41 nm and 52 nm, respectively. In addition, it can be seen that the particle size gradually grew with the reaction time, and then leveled off with the depletion of the monomers.

Zeta Potentials of Core–Shell Latex Particles

The magnitude of zeta potential gives an indication of the stability of the latex system. It is generally considered stable when the absolute value of the zeta potential exceeds 30 mV. If the zeta potential is a large negative or positive value, the particles will tend to repel each other instead of flocculation or coagulation. Figure 5(a) shows the effect of the surfactant amount on the zeta potential. It can be seen that the zeta potential reached a small magnitude of −23.3 mV when the amount of the surfactant was low (0.3 g SDS). Compared with the experiments

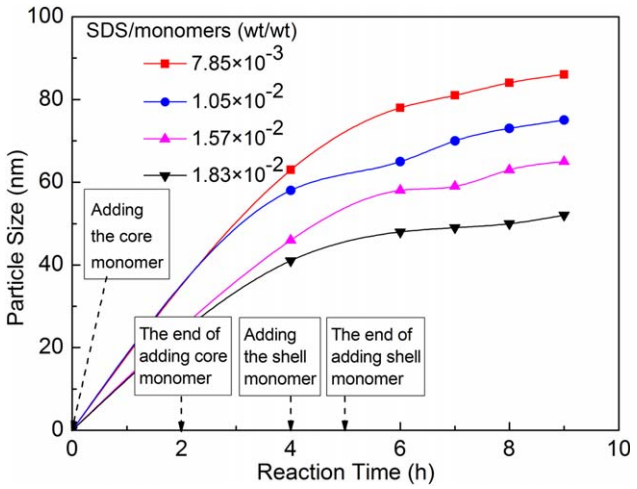

Figure 4. Particle sizes versus time with various weight ratio of surfactant/monomer (Core stage: 32 mL BA, 0.15 g KPS, 90 mL water, 80°C; Shell stage: 10 mL MMA, 0.05 g KPS dissolved in 10 mL of water, 80°C). [Color figure can be viewed in the online issue, which is available at wileyonlinelibrary.com.]

conducted with higher surfactant concentrations, the experiments with lower surfactant concentrations tended to have smaller zeta potential magnitudes and higher flocculation. The zeta potentials became large in the magnitude with the reduction of core or shell monomer amounts, as shown in Figure 5(b,c). The possible reason was that reducing the monomer amount led to decreased particle size, which increased the specific surface area (area of per unit volume) of the particles and allowed them to have more charges per unit weight of particles. More charges surrounding the particle surface led to higher zeta potentials, which also implied more stable latex.

Morphology of Particles

The TEM images in Figure 6(a,b) clearly show the well-defined core–shell latex morphology of particles. Figure 6(b) shows that PBA cores (the dark area) were surrounded by PMMA shells (the light area), which confirmed that the PBA-PMMA core–shell structures were formed via the differential microemulsion polymerization method. The average particle size (65 nm, particle size distribution index = 0.074) of core–shell latex measured by a dynamic light scattering mechanism based particle analyzer, Malvern Zetasizer Nano-ZS ZEN 3600 [Figure 6(c)] was in good agreement with the result of TEM.

Effect of Core/Shell Monomer Ratio on Mechanical Properties

The purpose of this work was not only to find the good reaction conditions in order to synthesize the acrylate based polymers with crease-whitening free properties, but also to achieve proper mechanical strength so that the resulting crease-whitening-free materials can be used as structure materials. Therefore, after synthesizing the acrylate based polymers with anti-crease-whitening, the investigation of the mechanical properties such as storage modulus (E'), loss modulus (E''), and loss factor (tan δ) follows below.

PBA-PMMA core–shell emulsions with different ratios of core–shell polymer (BA/MMA= 26/10, 28/10, 30/10, 32/10, and 34/10 mL/mL, which was labeled as a, b, c, d, and e, respectively in Figure 7) were directly coated on cleaned glass substrates, and dried to form 0.10 mm thick films at room temperature. As shown in Figure 7(a–c), for which a lower amount of the core monomer was used, significant cracks could be observed. However, when the core–shell monomer ratio was increased to 32/10, it formed a complete and transparent film as shown in Figure 7(d). That is because the increase in the BA amount resulted in the decrease in the glass transition temperature of the material, which had a direct effect on the film forming temperature. The scanning electron micrographs of the surface morphology about the complete film is shown in Figure 8, where a smooth surface without microvoids could be observed. However, when too much BA was used, the resulting polymer would lose the mechanical strength and become a soft coating without proper mechanical strength as shown in Figure 7(e), which was not desired. Therefore the mechanical properties were investigated as follows.

Dynamic mechanical properties of the two core–shell polymer film materials (BA/MMA= 32/10 and 34/10, labeled as a, b in Figure 9) such as storage modulus (E') and loss modulus (E'')

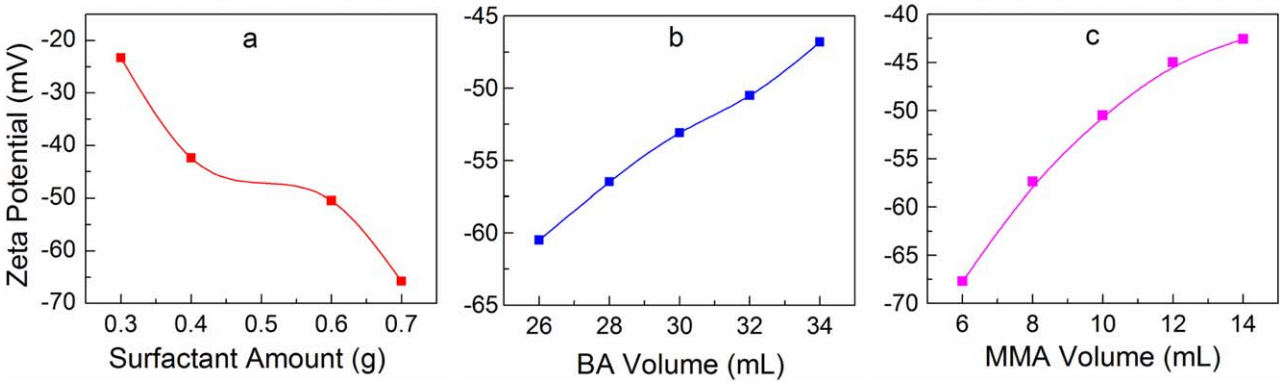

Figure 5. Zeta potentials of core–shell latex particles ((a) Core stage: 32 mL BA, 0.15 g KPS, 90 mL water, 80°C; Shell stage: 10 mL MMA, 0.05 g KPS dissolved in 10 mL of water, 80°C. (b) Core stage: 0.15 g KPS, 0.6 g SDS, 90 mL water, 80°C; Shell stage: 10 mL MMA, 0.05 g KPS dissolved in 10 mL of water, 80°C. (c) Core stage: 32 mL BA, 0.15 g KPS, 0.6 g SDS, 90 mL water, 80°C; Shell stage: 0.05 g KPS dissolved in 10 mL of water, 80°C). [Color figure can be viewed in the online issue, which is available at wileyonlinelibrary.com.]

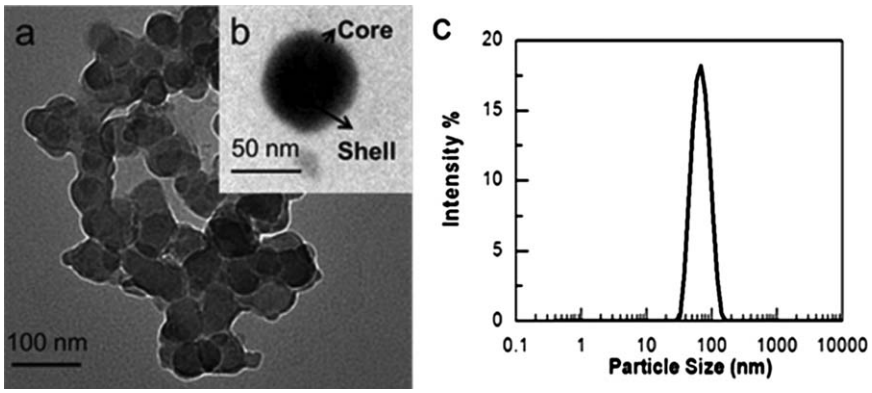

Figure 6. TEM images of core–shell particles (Core stage: 32 mL BA, 0.15 g KPS, 0.6 g SDS, 90 mL water, 80°C; Shell stage: 10 mL MMA, 0.05 g KPS dissolved in 10 mL of water, 80°C).

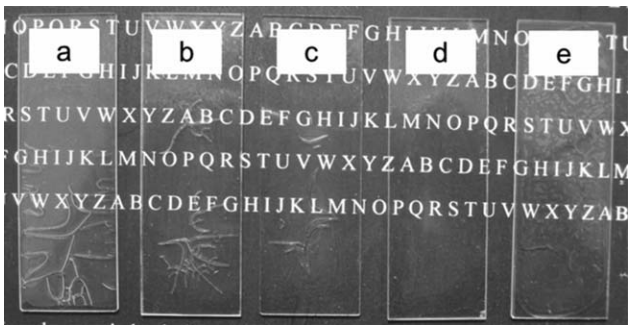

Figure 7. The images of films with different ratios of core/shell polymer (Core stage: 0.15 g KPS, 0.6 g SDS, 90 mL water, 80°C; Shell stage: 10 mL MMA, 0.05 g KPS dissolved in 10 mL of water, 80°C. Core stage, the amount of BA is (a) 24 mL; (b) 26 mL; (c) 28 mL; (d) 30 mL; (e) 32 mL).

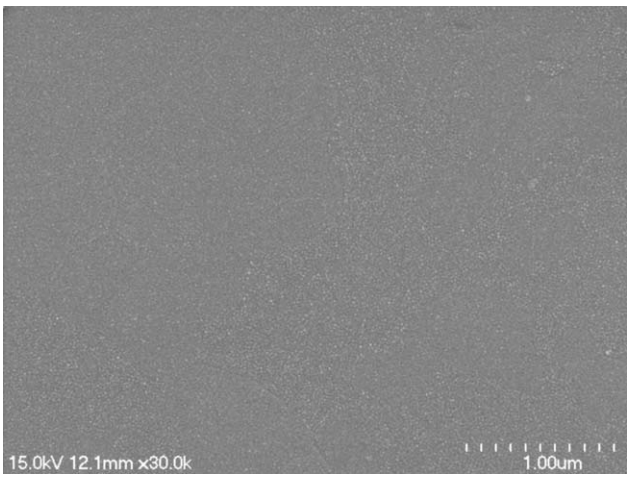

Figure 8. SEM morphology of film surface (Core stage: 32 mL BA, 0.15 g KPS, 0.6 g SDS, 90 mL water, 80°C; Shell stage: 10 mL MMA, 0.05 g KPS dissolved in 10 mL of water, 80°C).

of the core–shell polymers were measured and loss factor (tan δ) was evaluated. Storage modulus is a measure of the energy stored in the polymer, while the loss modulus is a measure of energy dissipated from the polymer during deformation. Storage modulus is related to the polymer elasticity, and loss modulus is related to its viscosity. The loss factor (tan δ) is equal to E''/E', reflecting the viscoelasticity of the core–shell polymer. Figure 9(a) showed that "a" with BA/MMA= 32/10 demonstrated a higher storage modulus than "b" with BA/MMA=34/10 at all the temperature region, which presented that "a" core–shell polymer film was more like elastomers than the "b". However, "b" core–shell polymer presented a higher loss modulus than "a" at −80°C to −20°C, as shown in Figure 9(b). It is obvious that core–shell polymer material with more soft components would reduce the rigidity. The tan δ values were plotted against

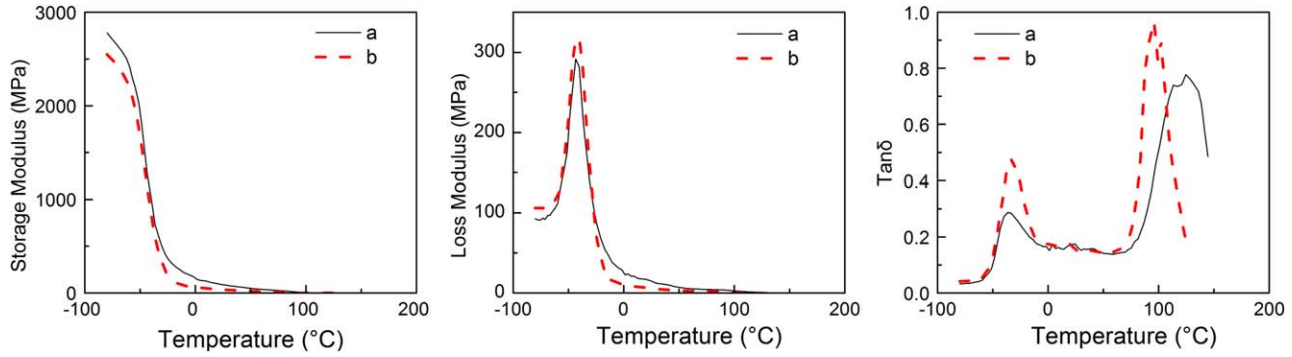

Figure 9. Dynamic mechanical analysis results of the core–shell polymer (Core stage: 0.15 g KPS, 0.6 g SDS, 90 mL water, 80°C; Shell stage: 10 mL MMA, 0.05 g KPS dissolved in 10 mL of water, 80°C). [Color figure can be viewed in the online issue, which is available at wileyonlinelibrary.com.]

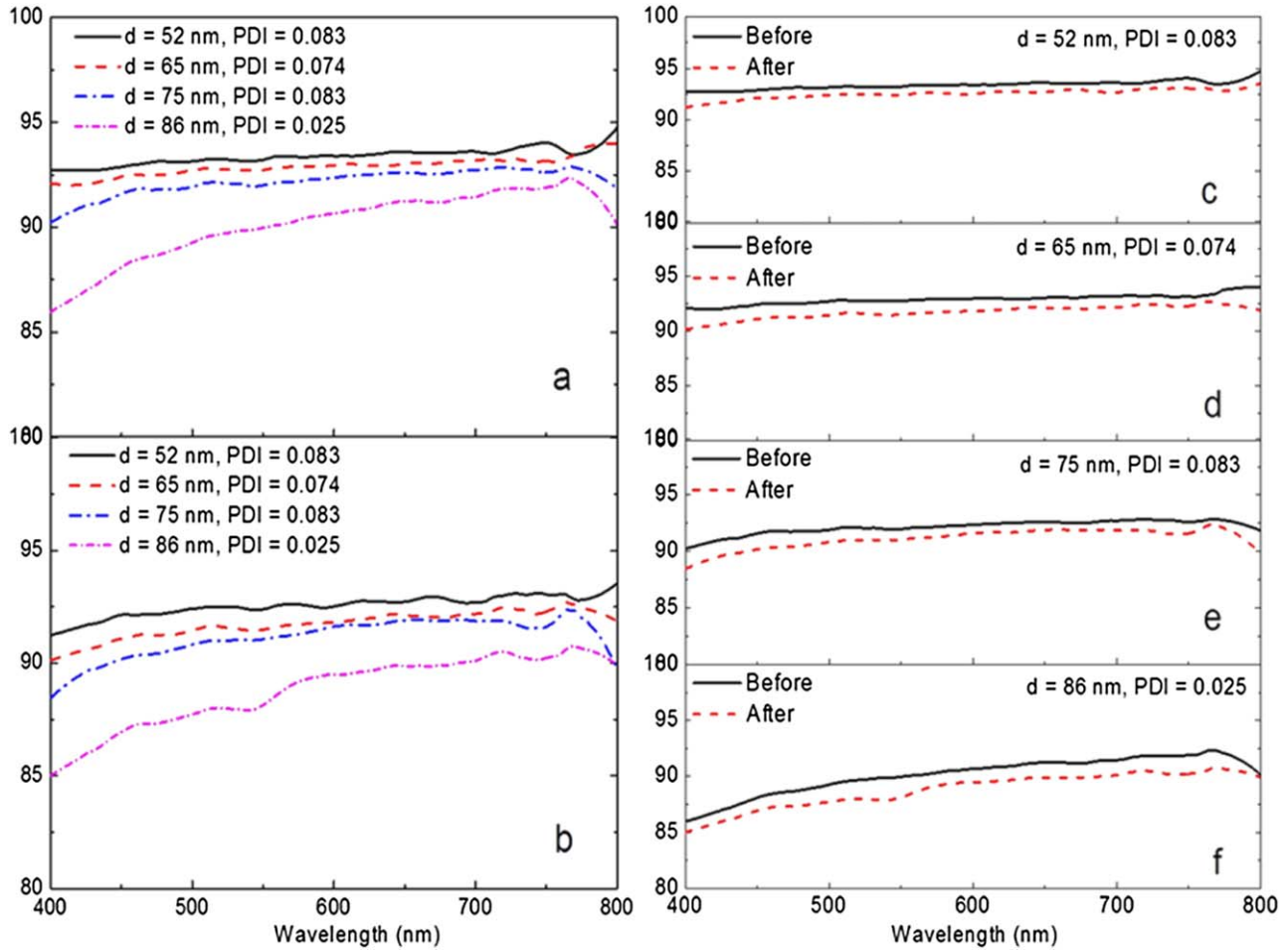

Figure 10. The transparency of films (a: the transparency of films with different particles size. b: the transparency of films after creasing. c–f: the transparency of each film before and after creasing). [Color figure can be viewed in the online issue, which is available at wileyonlinelibrary.com.]

temperature in Figure 9(c), which shows two peaks. This implied that the core–shell polymer had two glass transition temperatures, one at low temperature and another at high temperature region. Additionally, the glass transition temperatures of "b" core–shell polymer were lower than "a" core–shell polymer. It was also noticeable that the "b" maintained at a higher tan δ up to 100°C. The "b" core–shell material showed a rubbery behavior, while "a" core–shell polymer showed a hard and strong behavior that is required for being used as a structure materials.[50] Therefore, the amount of BA should be reduced in order to improve the mechanical properties of core–shell material. It would show soft, weak, and tack if the soft monomer was too much. In conclusion, the optimum core/shell monomer ratio was 32/10 (vol/vol) in these experiments.

Anti-Crease-Whitening Effect in Films

To study the anti-crease-whitening phenomenon, the effect of the particle size was further investigated with the optimized core/shell monomer ratios.

A number of films were made by the resulting polymers with various *Z*-average particles size (52, 62, 75, and 86 nm) in the method same as described above and each film had a dimension of about 60 mm × 20 mm × 0.1 mm. These films were folded[51] in half for five times and pressed by a weight of 100 g, which is approximately 26.7 kg/cm^2, for 24 h. The pressed films were then unfolded and measured via ultraviolet and visible spectrophotometer for their transmittance in the range of 400–800 nm before and after creasing. The results are shown in Figure 10. Figure 10(a) revealed that the films made with smaller particles had better transparency, and the minimum value of transparency increased from 86% to 93% when the particle size decreased from 86 to 52 nm. After creasing, as shown in Figure 10(b), the values of transparency showed negligible changes. As shown in Figure 10(c–f), the change in transmittance before and after creasing became smaller when the particle size was reduced. It means that film whitening phenomenon was insignificant. Thus it can be concluded that crease-whitening of films could be prevented by controlling the particle size and compositions.

CONCLUSIONS

PBA-PMMA core–shell nanoparticles were synthesized via differential emulsion polymerization with water-soluble initiator KPS and anionic surfactant SDS. Increasing the surfactant amount and raising the reaction temperature led to smaller particle sizes. The conversion and solid content were increased by raising the reaction

temperature. The resulting polymer films showed significantly improved anti-crease-whitening property with good mechanical properties when the BA/MMA monomer ratio for the core/shell structure was 32/10 (BA/MMA, vol/vol). The smaller the particle size the better the visible light transmittance.

ACKNOWLEDGMENTS

The authors gratefully acknowledge the support of the National Natural Science Foundation (No. 21176163), Suzhou Industrial Park and Soochow University. The authors would also like to thank Mr. Rob Reid at University of Waterloo, Canada, for editing the manuscript.

REFERENCES

1. Zhang, W.; Wang, Y.; Pan, M.; Rempel, G. L.; Pan, Q. *Plast. Ind.* **2012**, *40*, 1.
2. Yeosoo, J. S. O.; Yeosoo, S. K. N.; Yeosoo, O. Y. J. U.S. Pat. 6,855,786, B2, February 15, **2005**.
3. Liu, X.; Guo, M.; Wei, W. *Macromol. Symp.* **2012**, *312*, 130.
4. Dasari, A.; Misra, R. D. K. *Acta. Mater.* **2004**, *52*, 1683.
5. Hadal, R.; Yuan, Q.; Jog, J. P.; Misra, R. D. K. *Mater. Sci. Eng. A* **2006**, *418*, 268.
6. Pickering, K. L.; Sawpan, M. A.; Jayaraman, J.; Fernyhough, A. *Compos. A* **2011**, *42*, 1148.
7. Borthakur, L. J.; Jana, T.; Dolui, S. K. *J. Coat. Technol. Res.* **2010**, *7*, 765.
8. Bazilevsky, A. V.; Yarin, A. L.; Megaridis, C. M. *Langmuir* **2007**, *23*, 2311.
9. Lee, C. F.; Young, T. H.; Huang, Y. H.; Chiu, W. Y. *Polymer* **2000**, *41*, 8565.
10. Wang, Y.; Chen, L.; Liu, P. *Chem.—Eur. J.* **2012**, *18*, 5935.
11. Gonzalez-Leon, J. A.; Ryu, S. W.; Hewlett, S. A.; Ibrahim, S. H.; Mayes, A. M. *Macromolecules* **2005**, *8*, 8036.
12. Gui, Y.; Sun, S. L.; Han, Y.; Zhang, H. X.; Zhang, B. Y. *J. Appl. Polym. Sci.* **2010**, *115*, 2386.
13. Zhou, C.; Chen, M.; Zhang, M.; Zhang, H. *Polym. Bull.* **2007**, *59*, 699.
14. Chen, M.; Zhou, C.; Liu, Z.; Cao, C.; Liu, Z.; Yang, H.; Zhang, H. *Polym. Int.* **2010**, *59*, 980.
15. Jang, J.; Oh, J. H. *Adv. Funct. Mater.* **2005**, *15*, 494.
16. Berger, S.; Ionov, L.; Synytska, A. *Adv. Funct. Mater.* **2011**, *21*, 2338.
17. Mishra, S.; Singh, J.; Choudhary, V. *J. Appl. Polym. Sci.* **2010**, *115*, 549.
18. Zhou, C.; Che, R.; Zhong, L.; Xu, W.; Guo, D.; Lei, J. *J. Appl. Polym. Sci.* **2011**, *119*, 2857.
19. Lopez-Santiago, A.; Gangopadhyay, P.; Thomas, J.; Norwood, R. A.; Persoons, A.; Peyghambarian, N. *Appl. Phys. Lett.* **2009**, *95*, 143302.
20. Zhu, J.; Wei, S.; Ryu, J.; Sun, L.; Luo, Z.; Guo, Z. *ACS Appl. Mater. Interface* **2010**, *2*, 2100.
21. Li, Y. Q.; Fu, S. Y.; Yang, Y.; Mai, Y. W. *Chem. Mater.* **2008**, *20*, 2637.
22. Konwer, S.; Barthakur, L. J.; Dolui, S. K. *J. Mater. Sci. Mater. Electron.* **2012**, *23*, 837.
23. Viry, L.; Moulton, S. E.; Romeo, T.; Suhr, C.; Mawad, D.; Cook, M.; Wallace, G. G. *J. Mater. Chem.* **2012**, *22*, 11347.
24. Salehizadeh, H.; Hekmatian, E.; Sadeghi, M.; Kennedy, K. *J. Nanobiotechnol.* **2012**, *10*, 1.
25. Zhang, J. F.; Yang, D. Z.; Xu, F.; Zhang, Z. P.; Yin, R. X.; Nie, J. *Macromolecules* **2009**, *42*, 5278.
26. Hall, S. R.; Davis, S. A.; Mann, S. *Langmuir* **2000**, *16*, 1454.
27. Ni, K. F.; Sheibat-Othman, N.; Shan, G. R.; Fevotte, G.; Bourgeat-Lami, E. *Macromolecules* **2005**, *38*, 9100.
28. Ha, J. W.; Park, I. J.; Lee, S. B.; Kim, D. K. *Macromolecules* **2002**, *35*, 6811.
29. Sherman, R. L., Jr.; Ford, W. T. *Ind. Eng. Chem. Res.* **2005**, *44*, 8538.
30. Pusch, J.; van Herk, A. M. *Macromolecules* **2005**, *38*, 6909.
31. Guo, Y.; Wang, M.; Zhang, H.; Liu, G.; Zhang, L.; Qu, X. *J. Appl. Polym. Sci.* **2008**, *107*, 2671.
32. Okubo, M.; Minami, H.; Fujii, S.; Mukai, T. *Colloid Polym. Sci.* **1999**, *277*, 895.
33. Okubo, M.; Lu, Y.; Wang, Z. *Colloid Polym. Sci.* **1999**, *277*, 77.
34. Okubo, M.; Lu, Y. *Colloids Surf. A* **1996**, *109*, 49.
35. Yang, G.; Liu, Y.; Jia, R.; Xu, R.; Wang, X.; Ling, L.; Yang, J. *J. Appl. Polym. Sci.* **2009**, *112*, 410.
36. Mendrek, S.; Mendrek, A.; Adler, H. J.; Dworak, A.; Kuckling, D. *Macromolecules* **2009**, *42*, 9161.
37. Ohno, K.; Akashi, T.; Huang, Y.; Tsujii, Y. *Macromolecules* **2010**, *43*, 8805.
38. Schneider, G.; Decher, G. *Nano Lett.* **2004**, *4*, 1833.
39. He, G.; Pan, Q.; Rempel, G. L. *Macromol. Rapid. Commun.* **2003**, *24*, 585.
40. He. G.; Pan, Q. *Macromol. Rapid. Commun.* **2004**, *25*, 1545.
41. Liu, J.; Pan, Q. *J. Appl. Polym. Sci.* **2006**, *102*, 1609.
42. He, G.; Pan, Q.; Rempel, G. L. *J. Appl. Polym. Sci.* **2007**, *105*, 2129.
43. Norakankorn, C.; Pan, Q.; Rempel, G. L.; Kiatkamjornwong, S. *J. Appl. Polym. Sci.* **2009**, *113*, 375.
44. Norakankorn, C.; Pan, Q.; Rempel, G. L.; Kiatkamjornwong, S. *J. Appl. Polym. Sci.* **2010**, *16*, 1291.
45. Norakankorn, C.; Pan, Q.; Rempel, G. L.; Kiatkamjonwong, S. *Eur. Polym. J.* **2009**, *45*, 2977.
46. Zhang, X.; Wei, X.; Yang, W.; Li, Y.; Chen, H. *J. Coat. Technol. Res.* **2012**, *9*, 765.
47. Shultz, A. R. *J. Polym. Sci.* **1959**, *35*, 369.
48. Moghbeli, M. R.; Tolue, S. *J. Appl. Polym. Sci.* **2009**, *113*, 2590.
49. Udagama, R.; Mckenna, T. F. L. *J. Appl. Polym. Sci.* **2010**, *115*, 2668.
50. Ishak, Z. A. M.; Ishiaku, U. S.; Karger-kocsis, J. *J. Appl. Polym. Sci.* **1999**, *74*, 2470.
51. Strand, M. A.; Piner, R. L.; Salyer, D. G. U.S. Pat. 8,071,695, December 11, **2011**.